

Fatigue life of a microcantilever beam in bending

H. Hocheng,^{a)} K. S. Kao, and W. Fang

Department of Power Mechanical Engineering, National Tsing Hua University, Hsinchu 300, Taiwan, Republic of China

(Received 2 June 2004; accepted 27 September 2004; published 10 December 2004)

The fatigue behavior of a microcantilever beam loaded by various magnetic forces is investigated. The MEMS fabrication techniques, such as exposure, lithography, etching, etc., are applied to construct the micro structures on a silicon wafer. FEM and SEM are employed to study the relations between fractographies, stresses, and strains. The experimental results indicate that the deformation, stress and strain increase as the magnetic force increases, while the fatigue cycle time decreases with the load. The fatigue life lies in the range of $1-5 \times 10^7$ cycles at 12–15 MPa produced by the magnetic flux. Fracture occurs at the location of the maximum stress as predicted by an analytical approach. © 2004 American Vacuum Society. [DOI: 10.1116/1.1821502]

I. INTRODUCTION

Long-term reliability is essential for the successful application of MEMS. It is indispensable to study the mechanical properties associated with the lifetime of a MEMS device at the microscale level. The tensile and bending test,^{1–8} fracture test and fatigue analysis^{9–15} of microsamples and thin films were surveyed in the previous works. A 1 tensile testing method of thin films was proposed by Toshiyuki *et al.* using electrostatic forces. The free end of a cantilever beam is attached with the probe by an electrostatic force. The relationship between the displacement and the load reveals the mechanical properties of the structure. The mean tensile strength of each sample decreases with increasing specimen length. The mean tensile strength of a *p*-doped film is slightly lower than the nondoped films.² The electrostatic comb drive can also be used to generate the tensile force to the specimen. The result reveals that the aluminum film survived on a tensile stress of roughly 616 MPa, larger than the value obtained by Mearnini and Hoffman,³ about 180 MPa for freestanding films. Haque *et al.* reported that the yielding stress on the specimen at the beam support is about 880 MPa, 49 times larger than the bulk yielding stress of pure aluminum (55 MPa).⁴

Fracture strength varies with different etching chemicals used during fabrication processes.⁵ The fracture strength of the specimen etched by EDP is approximately twice that of the beam manufactured by KOH. Wilson *et al.* found the fracture strength, 3.3 GPa in average, is exceedingly larger than that of the back side, 1.0 GPa in average, because of the difference in the surface finish, where the front side of the beam was etched by reactive ion etching (RIE) and the back side of the beam was etched by potassium hydroxide (KOH) anisotropic etching.⁸

There are several approaches to observe the fatigue in MEMS. The failure occurs at various stress amplitudes,^{9–14} and the reduction of the stiffness^{12–15} and the changes of the resonant frequency^{9,13,16} also indicate the fatigue behavior. Muhlstein *et al.* used the electrostatic comb drive actuator to

apply the load to a notched cantilever beam. The results showed that the fatigue life in swinging motion ranged from about 10 s to 48 days, or 10^6-10^{11} cycles before failure over stress amplitudes ranging from approximately 4 to 10 GPa.¹⁰ Ando *et al.* performed tensile-mode fatigue testing of silicon films. The fracture point can be identified by observing the change in the load.¹¹ Schwaiger and Kraft studied the fatigue behavior of various Ag film thickness as on a SiO₂ cantilever beam. The mean stress levels ranged from 126 to 600 MPa and the damage was always observed after 3×10^6 cycles.^{13,14} The fracture occurs after the specimen has been tested for approximately 9864 s (2.74 h). A clear fatigue limit was not obtained in this study. The resonant frequency can also be applied to determine the fatigue life of the specimen. The drift of the resonant frequency indicates growth of the microdefect in a device. Muhlstein *et al.* observed that the resonant frequency decays with time due to the progressive decrease in the stiffness of the beam. The structure stiffness can also be adopted to define the fatigue life of the specimen. The stiffness decreases when fracture occurs at the interior of the structure.^{12,15–17} Li *et al.* used the nanoindenter to apply an oscillation load on a double clamped Si beam.¹² The sharp decrease in contact stiffness illustrate what fatigue damage has produced,^{12,15–17} approximately at 0.6×10^4 cycles.¹²

In this research,^{1–17} investigations on material properties, including fatigue, are performed subject to low-frequency loading, which deviates from many applications of MEMS devices. This paper reveals the fatigue behavior of a polysilicon beam subject to a high-frequency magnetic actuation and measured by a noncontact instrument. The results help explore the fatigue property of MEMS component and develop the test method for reliability standard.^{18–23}

II. THEORETICAL ANALYSIS OF FATIGUE

A. Sample and loading

The microcantilever beam is fabricated by bulk micromachining. The structure consists of two layers, a single crystal silicon layer and a magnetic film. The beam length is

^{a)}Electronic mail: hocheng@pme.nthu.edu.tw

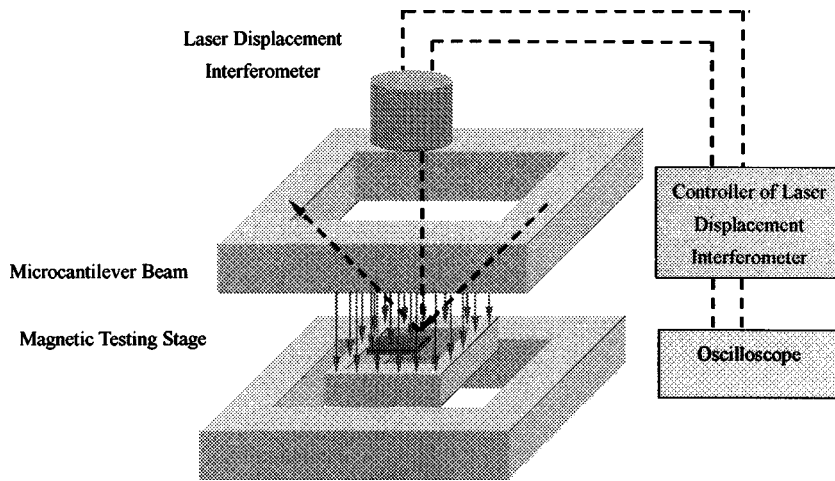


FIG. 1. Schematic of experimental set-up.

800 μm , the width is 100 μm , and thickness equals 20 μm . The loads are produced by magnetic circuits. The microstructure with a magnetic film in the magnetic field produces the magnetic forces which induce beam bending along the direction of magnetic field, as illustrated in Fig. 1. The magnetic energy can be expressed as a volume integral

$$U_m = \frac{1}{2} \int HBdv, \quad (1)$$

where H is magnetic intensity, B is magnetic flux density, v stands for volume, and $dv = S_m \cdot dy$. Hence

$$dU_m = \frac{1}{2} \frac{B^2}{\mu_0} S_m dy. \quad (2)$$

S_m is the area orthogonal to the magnetic field equal to the beam length (L) multiplied by the width (w), and μ_0 is the magnetic permeability in free space. The magnetic force is the derivative with respect to the y -coordinate

$$F_m = \frac{dU_m}{dy} = \frac{B^2}{2\mu_0} S_m. \quad (3)$$

B. Approach of mechanics of materials

Assuming the magnet force (F_m) is uniformly distributed on the beam surface, one can employ classic mechanics of materials to obtain the beam deflection induced by a uniform load (P) as

$$v = \frac{Px^2}{24EI} (6L^2 - 4Lx + x^2), \quad (4)$$

where L is the beam length, E is Young's modulus, and I is the moment inertia of the beam. The substitution of $P = (F_m/W) = (B^2 S_m / 2\mu_0 W)$ yields the maximum deflection at $x=L$,

$$v_{\max} = -\frac{B^2 L^5}{16EI\mu_0}. \quad (5)$$

The bending stress is derived by the classic mechanics of materials as

$$\sigma = -\frac{My}{I}, \quad (6)$$

where M is the bending moment

$$M = EI \frac{d^2v}{dx^2}. \quad (7)$$

Substituting Eq. (4) into Eq. (7), one obtains

$$M = -\frac{B^2}{48\mu_0} (12L^2 - 24Lx + 12x^2). \quad (8)$$

When $x=0$, the substitution of Eq. (8) into Eq. (6) yields the corresponding maximum bending stress

$$\sigma_{\max} = \frac{B^2 L^3 y}{4\mu_0 I}. \quad (9)$$

C. Approach of finite element method

Finite element methods can be utilized to analyze the deformation, stress, and strain when a uniform load is applied on the structure. This paper presents the relations between deformation, stress, strain, and the location of the maximum stress by ANSYS simulations. The boundary conditions in ANSYS are fixed and the uniform loading is applied on the surface of the beam.

D. Prediction of fatigue life

The fatigue life of a material can be described by Eq. (10)

$$\sigma_a = aN^b. \quad (10)$$

This expression is widely adopted for the experimental data of fatigue test. The fatigue life (N) is a function of the alternating stress σ_a . a and b are experimentally determined constants. Equation (10) can be rewritten as

$$N = \left(\frac{\sigma_a}{a} \right)^{1/b}. \quad (11)$$

The value of σ_a is equal to half of the maximum bending stress σ_{\max} . Substituting Eq. (9) into Eq. (11), one obtains

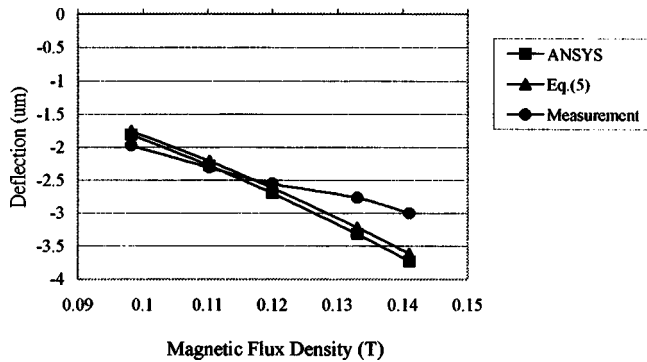


FIG. 2. Maximum deflection of microcantilever beam.

$$N = \left(\frac{B^2 L^3 y}{8 \mu_0 I a} \right)^{1/b} \quad (12)$$

III. EXPERIMENTAL METHOD

A. Experimental specimen

The bulk micromachining procedures, including lithography, exposure, etching, etc., are used to fabricate the structure of the microcantilever beam. A 1000 Å oxide film (SiO_2) is deposited on the silicon wafer followed by a 1500 Å nitride (Si_3N_4) film coated beyond the oxide as a passivation layer. The photoresist is then spin-coated on the wafer. Soft bake, in order to remove the solvent in the photoresist, is proceeded after coating. The following steps are to define the geometry of the beam by lithography, exposure and etching. The beam thickness is further patterned by the second mask. During the etching processes, KOH is used to determine the thickness. Afterwards, ICP is employed to etch through the thin film to release the microcantilever beam. The wafer is then cut to several pieces, each containing a microcantilever beam with a magnetic layer. The beam is finished as $800 \times 100 \times 20 \mu\text{m}^3$ in dimension.

B. Experimental set-up

The measuring facilities consist of a magnetic testing stage, a laser displacement meter, an oscilloscope, and a Gauss meter. The structure is fixed on the magnetic testing stage, where various magnetic fields apply the loads on the beam. The laser displacement meter is used to detect the beam deflection, as illustrated in Fig. 1. The deformation data can be used to calculate the beam stresses and to estimate the fatigue life. The fatigue test lasts about 7 days and the total cycle time of the fatigue life is around $1-5 \times 10^7$. Observations are made every 2 h to check if the cantilever beams break until the fatigue failure.

IV. RESULTS AND DISCUSSIONS

A. Deflection of microcantilever beam

The behavior of beam deflection is shown in Fig. 2. The beam deflection simulated by mechanics of materials and ANSYS increase as the magnetic flux density increases, as

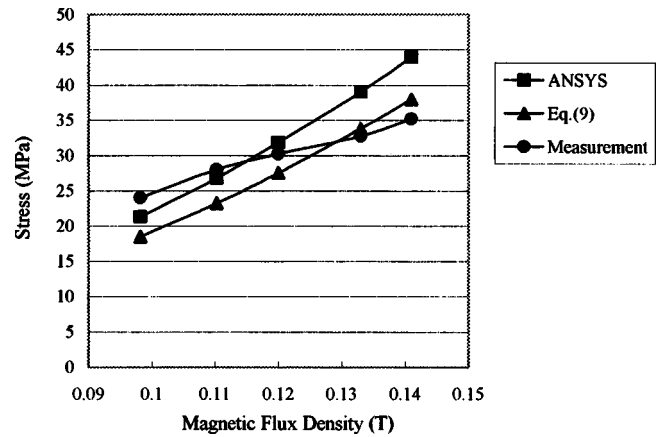


FIG. 3. Maximum stress of microcantilever beam.

shown in Eq. (5). The measured data increase the same with the magnetic flux. The less responsive deflection at a large magnetic load in the experiment can be attributed to the hysteric property of the magnetic film coated on the beam.

B. Stress of microcantilever beam

Figure 3 shows the maximum stress in the microcantilever beam similar to the deflection. The stresses predicted by the mechanics of materials and ANSYS increase as the magnetic flux density increases. The measured data increase also with the rise in magnetic flux. When the magnetic flux densities (B) are 0.098 T and 0.11 T, the measured data are slightly larger than the values calculated by mechanics of materials and ANSYS, about 12.6% and 4.5%, respectively. At 0.12 T, the measuring data are approximately equal to the ANSYS simulation and the predictions by material mechanics. As the magnetic flux densities increase to 0.13 T and 0.14 T, the measured data are smaller than the theoretical results of material mechanics calculation and ANSYS simulation, about 16% and 19.7%, respectively. The less responsive behavior of the beam is consistent with the results found in the deflection, and can be attributed to the hysteric magnetic film coated on the beam.

C. S–N fatigue curve of microcantilever beam

Figure 4 illustrates the S–N fatigue curve obtained in this study. The fatigue life decreases as the magnetic flux density increases. When the magnetic flux density is 0.098 T, the fatigue life of the microcantilever beam is 6 days and 15 hours, or 3.43×10^7 cycles in total, under the magnetic loading of ± 12 MPa. When the magnetic flux density increases to 0.11 T, the life of the beam lasts 5 days and 19 h or 3.0×10^7 cycles, under the loading of ± 14 MPa. At $B = 0.12$ T, the life becomes 5 days and 3 h, or 2.66×10^7 cycles, under the loading of ± 15 MPa. Based on the experimental results, the S–N fatigue curve of the beam is drawn in Fig. 4.

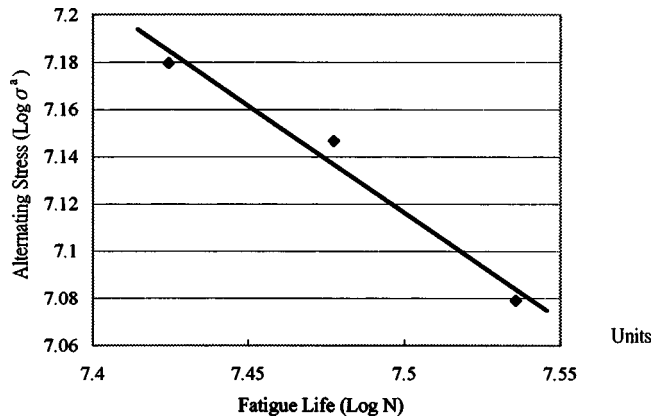


FIG. 4. Fatigue life of microcantilever beam.

D. Fractography

Figure 5 shows the fracture surface of the microcantilever beam. One finds that the surface is smooth and the fracture location does not occur at the root of the structure. Instead, it is located at $40 \mu\text{m}$ from the beam root. In the stress distribution of the beam obtained from the ANSYS analysis, the maximum bending stress does not occur at the root fillet, but appears at $40\text{--}50 \mu\text{m}$ away from the root. The fracture location found in the experiment agrees with predicted location of the maximum bending stress.

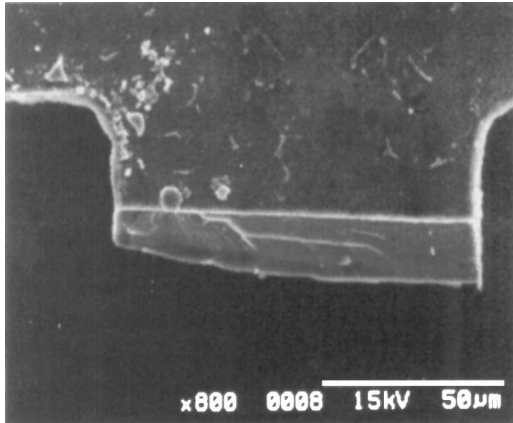


FIG. 5. Fatigue fractography of microcantilever beam.

V. CONCLUSIONS

Based on the results of analytical predictions, simulations and the experiment described above, the following conclusions are drawn. The deformation, stress, and strain increase as the magnetic flux density rises, while the fatigue life of the microcantilever beam shortens when the magnetic flux density increases. The beam life is expected to be $1\text{--}5 \times 10^7$ cycles at the stress level of $12\text{--}15 \text{ MPa}$ produced by the magnetic flux. The experimental data shows a lower level of response to the magnetic flux than the theoretical analysis when the loading is high, which can be attributed to the coated magnetic film on the specimen. Fracture occurs at the location of the maximum stress as predicted by ANSYS.

ACKNOWLEDGMENT

The current research was supported by the National Science Council, Taiwan, ROC, under Contract No. NSC92-2212-E007-050.

- ¹K. P. Larsen *et al.*, *Sens. Actuators, A* **103**, 156 (2003).
- ²T. Tsuchiya *et al.*, *J. Microelectromech. Syst.* **7**, 106 (1998).
- ³G. T. Mearmini and R. W. Hoffman, *J. Electron. Mater.* **22**, 623 (1993).
- ⁴M. A. Haque *et al.*, *J. Microelectromech. Syst.* **10**, 146 (2001).
- ⁵T. Yi *et al.*, *Sens. Actuators B* **83**, 172 (2000).
- ⁶P. T. Jones, G. C. Johnson, and R. T. Howe, *Micromechanical Structures for Fracture Testing of Brittle Thin Films*, Proc. MEMS, DSC-Volume 59, ASME Int. Mechanical Engineering Congress and Exposition, Atlanta, GA, November 1996, pp. 325–330.
- ⁷T. Yi and C. J. Kim, *Meas. Sci. Technol.* **10**, 706 (1999).
- ⁸C. J. Wilson *et al.*, *J. Appl. Phys.* **79**, 2386 (1996).
- ⁹Christopher *et al.*, *J. Microelectromech. Syst.* **10**, 593 (2001).
- ¹⁰C. L. Muhlstein *et al.*, *Sens. Actuators, A* **94**, 177 (2001).
- ¹¹T. Ando *et al.*, *Sens. Actuators, A* **93**, 70 (2001).
- ¹²X. D. Li *et al.*, *Surf. Coat. Technol.* **163–164**, 521 (2003).
- ¹³O. Kraft *et al.*, *Mater. Sci. Eng., A* **319–321**, 919 (2001).
- ¹⁴R. Schwaiger and O. Kraft, *Acta Mater.* **51**, 195 (2003).
- ¹⁵W. N. Sharpe Jr. and J. Bagdahn, *Mech. Mater.* **36**, 3 (2004).
- ¹⁶G. T. A. Kovacs, *Micromachined Transducers Sourcebook* (McGraw-Hill, New York, 1998).
- ¹⁷C. T. Gibson *et al.*, *Ultramicroscopy* **97**, 113 (2003).
- ¹⁸G. P. Zhang, K. Takashima, M. Shimojo, and Y. Higo, *Mater. Lett.* **57**, 1555 (2003).
- ¹⁹P. T. Jones, G. C. Johnson, and R. T. Howe, in Proc. MEMS, Dsc-Volume 59, ASME Int. Mechanical Engineering Congress and Exposition, Atlanta, GA, November 1996, pp. 325–330.
- ²⁰K. E. Petersen, *IEEE Trans. Electron Devices* **ED-25**, 1247 (1978).
- ²¹G. T. A. Kovacs, Nadim I. Maluf, and Kurt E. Petersen, *Proc. IEEE* **86**, 1536 (1998).
- ²²Gere and Timoshenko, *Mechanics of Materials*, 4th ed. (International Thomson, New York, 1997).
- ²³K. E. Petersen, *Proc. IEEE* **70**, 420 (1982).